Four-wave mixing in potassium vapor with an off-resonant double-Λ system

M. M. Ćurčić*
Institute of Physics Belgrade, University of Belgrade, Pregrevica 118, 11080 Belgrade, Serbia
and School of Electrical Engineering, University of Belgrade, Bulevar kralja Aleksandra 73, 11120 Belgrade, Serbia

T. Khalifa, B. Zlatković, I. S. Radojičić, A. J. Krmpot, D. Arsenović, and B. M. Jelenković
Institute of Physics Belgrade, University of Belgrade, Pregrevica 118, 11080 Belgrade, Serbia

M. Gharavipour
Laboratoire Temps-Fréquence (LTF), Institut de physique, Université de Neuchâtel, Neuchâtel CH-2000, Switzerland

(Received 5 October 2017; revised manuscript received 26 March 2018; published 25 June 2018)

We investigate both theoretically and experimentally four-wave mixing (FWM) in hot potassium vapor, generated by a copropagating pump and probe in an off-resonant double-Λ system, and present conditions when this atomic system is (1) a strong phase-insensitive parametric amplifier and (2) a source of large-amplitude squeezing. Theoretically, nonperturbative numerical calculations of optical Bloch-Maxwell equations have been solved for a four-level atomic system of K in order to derive the atomic polarization and then amplitudes of propagating optical waves, pump, probe, and conjugate. For potassium, to our knowledge, there are no such comparisons of theoretical and experimental results of gains of twin beams under the large range of FWM parameters as presented here. Results have shown that one-photon detuning has to be slightly larger than the Doppler broadened transition for large gains and strong squeezing. The gain is particularly large for small red two-photon detuning (−2–6 MHz) and high K density (5.5–10 × 10^{12} cm^{-3}). Following experimentally and theoretically determined relation between gains, probe transmissions, and squeezing in Rb and Cs, we have found parameters of FWM when maximum squeezing in hot K vapor is expected.

DOI: 10.1103/PhysRevA.97.063851

I. INTRODUCTION

Four-wave mixing (FWM) is a nonlinear phenomenon that in alkali-metal vapors can efficiently generate entangled photon pairs, essential for probing quantum properties of light and for quantum information [1–3]. It also enables slowing and storing of light in atomic ensembles [4–9], essential elements for quantum memories.

Different schemes have been used to generate paired photons, such as on-resonant spontaneous FWM [2], the diamond [10], and double ladder scheme FWM [11]. An atomic system that is often used for generation of twin beams is off-resonant FWM in a double-Λ scheme, realized by two input fields, pump and probe, in a three (four) -level atomic system. The lower Λ is made of pump and probe photons, while the pump photon and conjugate photon close the upper Λ (see Fig. 1). This atomic scheme is similar to schemes for electromagnetically induced transparency (EIT) and becomes nonlinear FWM under certain conditions: whether the system will behave like EIT or a parametric amplifier depends on laser detunings, atomic density, and pump power [12,13]. While resonant absorption processes for EIT conditions lead to losses, FWM gains of both probe and conjugate, typically observed for high pump beam, allow for much larger propagation distances [4,14,15].

A nondegenerate, off-resonant double-Λ scheme was found to be a good source for relative amplitude squeezing [16–19] and for simultaneously generated intensity correlations and phase anticorrelations or entanglement of probe and conjugate [20,21]. Large entanglement is an important resource for quantum information [22]. A correlation between the amount of squeezing and entanglement and the gain of the twin beam is established [20].

Theoretically, FWM was studied in degenerate and counterpropagating laser beams [23], as well as in nondegenerate and copropagating beams. In the latter, nonlinear parametric processes in FWM were studied in a double-Λ configuration with either resonant (larger contribution from CPT and EIT phenomena) [24] or off-resonant pump frequency [15], in hot gas vapors or in cold atoms [25]. There are different approaches to model complex processes in FWM. They depend on the intended applications of the system, which can be parametric gain, quantum-correlations of twin beams, squeezing and entanglement, slow and stored light, i.e., whether classical or quantum properties are of interest. For work presented here, the most relevant are models that analyze the continuous wave regime and calculate gains of twin beams. Quantum mechanical theory of multiwave mixing was applied for calculating Rabi sidebands generated by FWM [26]. In most models, the treatment is based on analytical solutions, after perturbation theory and a number of approximations being applied [15]. In the seminal paper [24], pump and probe are resonant with atomic transitions with conditions for EIT, while

*marijac@ipb.ac.rs

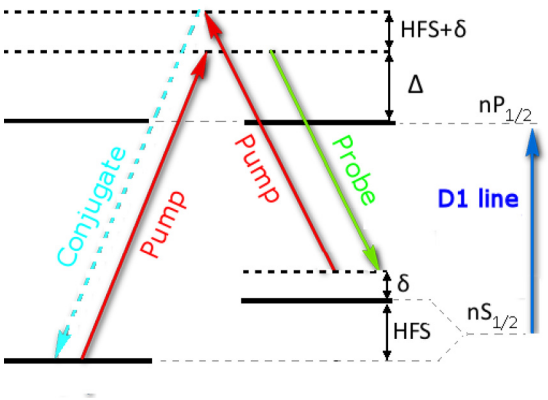

FIG. 1. Double Λ scheme at D_1 line of an alkali-metal atom. hfs = hiperfine splitting, Δ = one-photon detuning, δ = two-photon detuning. Levels: $|1\rangle$ and $|2\rangle$ = hyperfine levels of $4S_{1/2}$, $F = 1$ and $S_{1/2}$, $F = 2$ respectively, $|3\rangle = 4P_{1/2}$, $|4\rangle$ = virtual level, degenerate with $|3\rangle$, introduced by the model. Hfs of the level $|3\rangle$ is negligible in comparison with ground state hfs.

cross susceptibilities are enhanced by coherence in the ground hyperfine levels. Heisenberg-Langevin formalism was used to calculate the classical and quantum properties of probe and conjugate beams beyond the linear amplifier approximation [25,27]. A phenomenological approach when the medium is quantum mechanically described by a simple model of distributed FWM gain and probe loss was used in Ref. [16].

FWM in alkali metals has been extensively studded, particularly in Rb and Cs [4,14,16,19,25,28,31], but little work was done on potassium [32–37]. Potassium has hyperfine splitting (hfs) of the ground state of only 460 MHz, by far smaller then for any other alkali metal. For FWM based on two pump photons, small hfs means that detuning of the upper Λ scheme is not far from detuning of the lower Λ scheme. This suggests that large gains and squeezing and other FWM properties are possible at lower laser power.

With this study, we extend our previous work on FWM in K [33] with results of the theoretical model and new experimental results. The model is a semiclassical treatment of FWM processes, and atomic polarization, calculated from optical Bloch equations (written for the system presented schematically in Fig. 1), is applied in the propagation equations to obtain amplitudes of three optical fields at the exit from the K vapor. We compare calculated and measured gains for a wide range of parameters, which is important for efficiency of FWM. This includes the angle between the pump and the probe, atomic density, detuning of the pump from the D_1 transition, Δ, and two-photon detuning in respect to hfs of the ground state, δ.

Performance of FWM for high-level squeezing, quantum information protocols, and quantum cloning machines [3] strongly depends on FWM parameters: vapor density, Δ and δ. The former controls probe absorption, while two detunings control nonlinearity and gain. Measurements and models [16,18] have shown that for stronger squeezing and low noise figures, moderate gains of probe and conjugate are at a maximum, while probe absorption is minimal. We made intensive calculations of gains and probe transmissions for the large range of K density and one- and two-photon detuning, and present parameters of FWM that we believe will generate the strongest quantum correlations and squeezing in K vapor. In the theoretical analyses for FWM parameters for strong squeezing we have included results that take into account the Doppler average of density matrix elements. These values are compared with values used in a resent experiment [38] to measure squeezing in K vapor. Since for the alkali-metal atoms with higher hyperfine splitting of the ground state, higher powers are required for efficient degree of squeezing [19,29], we believe that potassium, having the smallest hfs of the ground state, could be more convenient, compared to others, for high-level amplitude squeezing.

II. THEORETICAL MODEL

In the model, the three electric field modes, pump (drive), probe, and conjugate, with frequencies ω_d, ω_p, and ω_c, respectively, interact with four levels of the ^{39}K atom. The double-Λ scheme with modes coupling atomic levels of the D_1 transition is given in Fig. 1. Level $|3\rangle$ is $4P_{1/2}$, while levels $|1\rangle$ and $|2\rangle$ are hyperfine levels of $4S_{1/2}$, $F = 1$ and $F = 2$, respectively. The lower Λ scheme consists of the pump photon that couples the level $|1\rangle$ to the level $|3\rangle$ with the one-photon detuning $\Delta_{(13)} = \Delta$. The other "leg" of the first Λ scheme is the probe photon that stimulates the Stokes scattering from level $|3\rangle$ to the level $|2\rangle$, with two-photon detuning $\Delta_{(132)} = \delta$. The pump is sufficiently strong to drive the off-resonant transition $|2\rangle \rightarrow |4\rangle$ in the upper Λ scheme. By the way of stimulating anti-Stokes scattering the conjugate photon closes the upper scheme. The total detuning for the level $|4\rangle$ is $\Delta_{(1324)} = (2\omega_d - \omega_p) - (\omega_4 - \omega_1)$, where $\omega_4 - \omega_1$ is angular frequency of the transition $|1\rangle \rightarrow |4\rangle$. We introduce level $|4\rangle$, which is degenerate to the level $|3\rangle$, and like level $|3\rangle$ is weakly coupled to both level $|1\rangle$ and level $|2\rangle$ because of a large detuning.

Atoms are simultaneously illuminated by the pump, probe, and conjugate and experience a total electric field approximated by the sum of three monochromatic fields:

$$\mathbf{E} = \sum_{i=d,p,c} \mathbf{e}_i E_i^{(+)} e^{-i\omega t + i\mathbf{k}_i \mathbf{r}} + \text{c.c.} \tag{1}$$

Here $E^{(+)}$ is the slowly varying approximation of the fields envelope, at positive frequencies. The Hamiltonian for the atomic system is given by

$$\hat{H} = \hat{H}_0 + \widehat{H_{\text{int}}} = \sum_{i=1}^{4} \hbar\omega_i |i><i| - \hat{\mathbf{d}} \cdot \mathbf{E}(\mathbf{r},t), \tag{2}$$

where $\hat{H}_0$ is the unperturbed Hamiltonian of the system and $\widehat{H_{\text{int}}}$ is interaction Hamiltonian, $\hbar\omega_i$ is the energy of atom level i, and $\hat{\mathbf{d}}$ is atomic dipole moment.

Atomic dynamics is described by the set of Bloch equations for density matrix elements $\hat{\rho}$:

$$\dot{\hat{\rho}} = -\frac{i}{\hbar}[\hat{H},\hat{\rho}] + \widehat{SE} + \hat{R}, \tag{3}$$

where $\widehat{SE}$ denotes the spontaneous emission from the excited states, and $\hat{R}$ is the relaxation due to atom transit time-induced losses and collisional dephasing. The full set of Eq. (3) is given in the Appendix. Because of the fast oscillating laser field, as

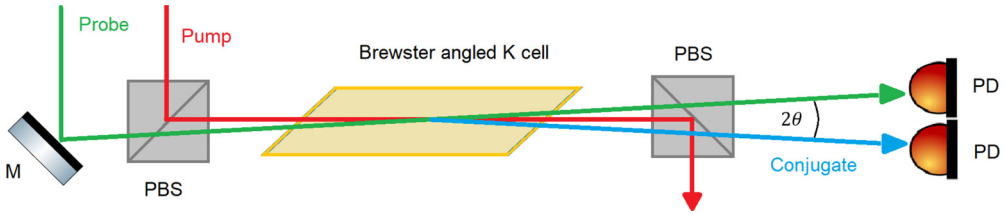

FIG. 2. Experimental setup. M = mirror, PBS = polarization beam splitter, PD = photodetector.

in Eq. (1), substituting H from Eq. (2) into Eq. (3) produces fast oscillating terms in ρ_{ij}. After substitution,

$$\tilde{\rho}_{ij} = e^{-i\omega_{(ij)}t + i\mathbf{k}_{(ij)}\mathbf{r}}\rho_{ij}, \tag{4}$$

where $\omega_{(ij)}$ are different angular frequencies: $\omega_{(13)} = \omega_{(24)} = \omega_d$, $\omega_{(23)} = \omega_p$, $\omega_{(14)} = \omega_c$, $\omega_{(12)} = \omega_{(13)} - \omega_{(23)}$, $\omega_{(34)} = \omega_{(14)} - \omega_{(13)}$, $\omega_{(ij)} = -\omega_{(ji)}$, and $\mathbf{k}_{(ij)}$ are wave vectors of sums (differences) of wave vectors: $\mathbf{k}_{(13)} = \mathbf{k}_{(24)} = \mathbf{k}_d$, $\mathbf{k}_{(23)} = \mathbf{k}_p$, $\mathbf{k}_{(14)} = \mathbf{k}_c$, $\mathbf{k}_{(12)} = \mathbf{k}_{(13)} - \mathbf{k}_{(23)}$, $\mathbf{k}_{(34)} = \mathbf{k}_{(14)} - \mathbf{k}_{(13)}$, $\mathbf{k}_{(ij)} = -\mathbf{k}_{(ji)}$ with $\mathbf{k}_c = 2\mathbf{k}_d - \mathbf{k}_p - \Delta\mathbf{k}$. Terms that oscillate with the sum of frequencies are neglected in the rotating wave approximation. Left in Eq. (3) are time-independent terms and a few spatially dependent terms with oscillating coefficients $e^{i\Delta kz}$.

Propagation along the z direction and temporal evolution of pump, probe, and conjugate are described by the set of nonlinear equations for the slowly varying envelopes of the three fields:

$$\left(\frac{\partial}{\partial z} + \frac{1}{c}\frac{\partial}{\partial t}\right)E_d^{(+)} = i\frac{kN}{2\varepsilon_0}d(\tilde{\rho}_{(42)} + \tilde{\rho}_{(31)}), \tag{5a}$$

$$\left(\frac{\partial}{\partial z} + \frac{1}{c}\frac{\partial}{\partial t}\right)E_p^{(+)} = i\frac{kN}{2\varepsilon_0}d\tilde{\rho}_{(32)}, \tag{5b}$$

$$\left(\frac{\partial}{\partial z} + \frac{1}{c}\frac{\partial}{\partial t}\right)E_c^{(+)} = i\frac{kN}{2\varepsilon_0}d\tilde{\rho}_{(41)}. \tag{5c}$$

Here N is the atom density.

Since we are also interested in probe absorption, we calculate the above equations by setting the intensity of pump beam to be zero. The probe transmission is then the quotient of the intensities of the outgoing and incoming probe beam. In a hot vapor the Doppler effect is present. The shift of the observed angular frequency is dependent on the z component of the velocity, v_z, for which the Maxwell distribution is given by

$$f(v_z) = \sqrt{\frac{m}{2\pi kT}}e^{\frac{-mv_z^2}{2kT}}, \tag{6}$$

The observed angular frequency is $\omega_0 = \sqrt{\frac{1-\beta}{1+\beta}}w_s$, where ω_s is angular frequency of the source and $\beta = v/c$. The frequency shift alters one photon detuning and detuning of the conjugate pulse, while two-photon detuning stays the same since the pump and probe are almost copropagating. Hence, density matrices depend on v_z. We perform Doppler averaging with the most basic approximation. We calculate the signals, gains of twin beams, and probe transmission for different v_z and then average them over the Maxwell distribution.

The gains of the probe (conjugate) are calculated from the ratio of amplitudes of probe (conjugate) at the exit from the K vapor to the probe amplitude at the entrance to the vapor. The model assumes that the pump and the probe fully overlap. The gas cell used in the experiment is 5 cm long, therefore for a typical angle between the probe and the pump ∼3 mrad, beams are overlapped only in the part of the cell. Our theoretical results are for a 1 cm long interaction region. Parameters used in the calculations are as in the experiment, like atom density, one- and two-photon detuning, and angle between pump and probe. Rabi frequencies of the pump and probe are calculated from the laser intensity I using $\Omega = \frac{2dE_0^{(+)}}{h}$, $E = E_0\cos(\omega t) = E_0^{(+)}e^{-i\omega t} + E_0^{(-)}e^{i\omega t}$, $E_0^{(+)} = \frac{E_0}{2} = \sqrt{(\eta I/2)}$. Here $\eta = 376.73\ \Omega$ [39] is the vacuum impedance, and d is the reduced dipole matrix element, which for potassium is $d = 1.74 \times 10^{-29}$ Cm [40]. For total relaxation rates, γ (see the Appendix), we used the value $\gamma \sim 10^5$ Hz.

III. EXPERIMENT

We have measured gains of the probe and the conjugate using the setup described in Ref. [33]; see Fig. 2. Laser beam from the high-power, narrow line laser (Coherent, MBR 110) is split in two by a 90:10 beam splitter. A stronger beam is used as the pump beam, and the weaker fraction is the probe beam. The probe is sent through two AOMs, one in a double pass, for the probe frequency detuning in respect to the pump frequency, and for scanning of this detuning around the hfs of the K ground state. Thus, we vary two-photon detuning δ by changing the probe frequency and vary one-photon detuning Δ by tuning the pump frequency. Diameters of the pump and the probe beams are 1.1 mm, and 0.75 mm, respectively. Two beams are orthogonally polarized and recombined on the polarizing beam cube before entering the K cell. This is the vacuum K cell with natural abundance of isotopes, 5 cm long, 25 mm in diameter. The cell was heated by hot air up to 150 °C. Pump and probe beams enter the cell at the small angle θ. We can adjust this angle by changing the probe direction with the entrance mirror, placed before the combining cube. With the pump beam behind the cell blocked, two beams emerge: probe and the frequency up-shifted beam (conjugate). Both beams are detected with the pair of photodetectors. We get the gains of the probe and the conjugate from the ratios of measured powers of the probe and conjugate beams behind the cell to the probe beam input power. Radius and shape of beams behind the cell are monitored with a CCD beam profiler.

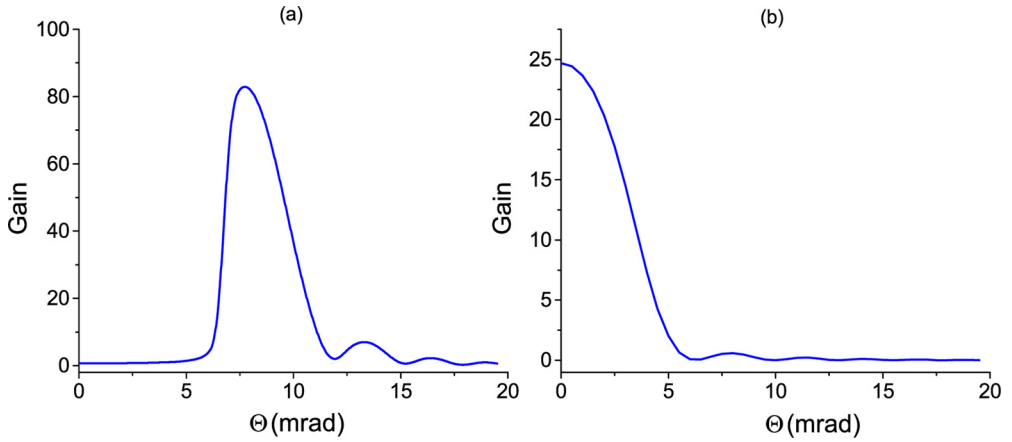

FIG. 3. Calculated gain of the conjugate beam as a function of the angle θ for two pump powers. (a) $\Omega_d = 3.25$ GHz, (b) $\Omega_d = 1.95$ GHz, for $N = 1 \times 10^{12}$ cm^{-3}, $\delta = -9.5$ MHz, $\Delta = 1$ GHz, and $\Omega_p = 22.5$ MHz.

IV. RESULTS AND DISCUSSION

In this section we present results of gains of twin beams as a function of FWM parameters: the angle between the pump and the probe, gas density, one- and two-photon detuning, and the probe power. But, as we will show, dependence on one of the parameters depends on values of the other parameters.

A. Measured and calculated gains of probe and conjugate

1. Dependence of gains on the angle between pump and probe

Probe and conjugate gains as a function of the angle θ between the pump and the probe are results of FWM phase matching. As we see from results in Figs. 3 and 4, the phase matching condition is satisfied at different angles θ, depending on values of other parameters. Behavior of FWM gains versus θ is influenced by the index of refraction at the probe frequency, which is influenced by values of laser powers, densities, and detunings. In Figs. 3 and 4 we present calculated conjugate beam gains as a function of θ. We decided not to show results for the probe because the model gives very similar behavior of gains of the probe and the conjugate.

Results in Fig. 3 are obtained for different pump Rabi frequencies, while results in Fig. 4 are for different density of the K vapor. Results show that FWM gains have different behavior at high and low pump Rabi frequencies Ω_d (Fig. 3) and at high and low K densities (Fig. 4). In both figures, one- and two-photon detunings, and probe Rabi frequency Ω_p are $\Delta = 1$ GHz, $\delta = -9.5$ MHz, and $\Omega_p = 22.5$ MHz. As we can see, at high Ω_d and higher density, FWM gains are in a narrow range of angles θ and the gain maximum is away from zero values of δ. On the other hand, at lower power and density, FWM phase matching is found at smaller angles. Here gain increases as θ is decreasing. Occurrence of FWM gains at near zero angle means negligible changes of index of refraction at the probe frequency and/or its continuous change along the vapor due to strong pump absorption and therefore variation of pump power along the propagation direction. The possibility of the latter was not supported by the calculated pump absorption. On the other hand, our model shows correlation between how gain depends on angle, and the amount of the phase changes of the probe and conjugate. When the gain versus angle is a narrow peak as in Fig. 3(a), then Δk_z varies for more then 2π over the propagated distance. When gain monotonically changes as the angle increases from zero, Δk_z changes only a little, less then $\pi/4$.

Experimental results for the gains of twin beams as a function of the angle θ for K densities of 5.5×10^{12} cm^{-3} (cell temperature 130 °C) and 1.75×10^{13} cm^{-3}(150 °C) are given in Fig. 5. The smallest value of the angle between pump and probe we needed to separate the probe and conjugate

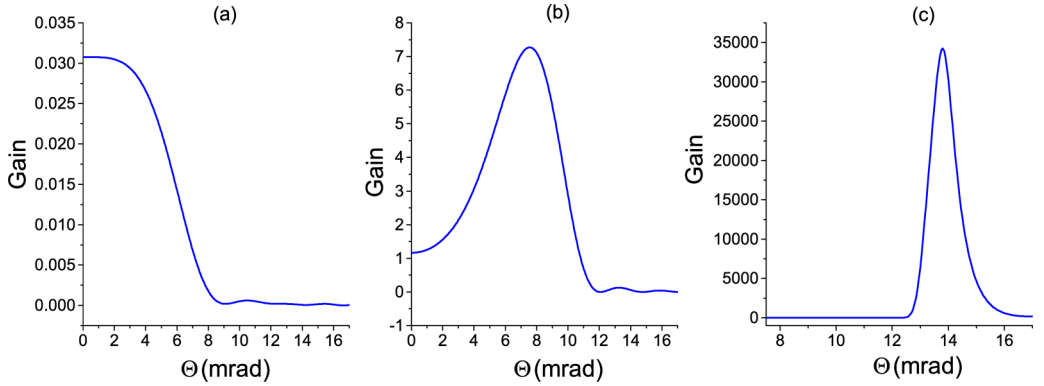

FIG. 4. Calculated gain of the conjugate beam as a function of the angle θ, for three values of the potassium density. (a) $N = 1 \times 10^{13}$ cm^{-3}, (b) $N = 1 \times 10^{12}$ cm^{-3}, and (c) $N = 1 \times 10^{11}$ cm^{-3} for $\Omega_d = 1.95$ GHz, $\Omega_p = 22.5$ MHz, $\delta = -9.5$ MHz, and $\Delta = 1$ GHz.

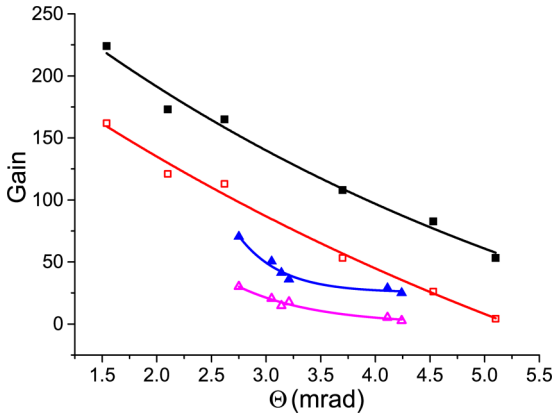

FIG. 5. Experimental results of gains of probe (open symbols) and conjugate (filled symbols) for two K density, $5.5 \times 10^{12}\,\mathrm{cm}^{-3}$ (squares) and $1.7 \times 10^{13}\,\mathrm{cm}^{-3}$ (triangles). $\Delta = 1\,\mathrm{GHz}$ (for lower density) and 1.35 GHz (for higher density). $\delta = -3.7\,\mathrm{MHz}$, $P_d = 370\,\mathrm{mW}$, and $P_p = 25\,\mu\mathrm{W}$.

behind the cell was $\theta = 1.5$ mrad. The twin beam gains at the highest vapor density that we had in the experiment are lower and were measured only at high $\Delta = 1.35\,\mathrm{GHz}$. Experimental results of gains versus angle, as shown in Fig. 5, are typical for copropagating pump and probe with a similar diameter in a rather long gas cell, because beams do not fully overlap in parts of the cell.

2. Dependence of gains on two-photon detuning

Calculated and measured gains of the probe and the conjugate versus two-photon detuning δ, for several values of one-photon detuning, are presented in Fig. 6. Dependence is given for two Δ, 1 GHz and 1.35 GHz, and for $\theta = 5.5$ mrad. Typical widths of calculated gains are between 1.5 and 3 MHz, and of measured gains are 6–13 MHz.

Maximum of gains are, at δ_m, shifted from two-photon resonance ($\delta \approx 0$). This shift is mainly due to differential Stark shift, δ_S, because of different detunings of hyperfine levels from the off-resonant pump. As shown in Fig. 6, δ_m is larger for smaller Δ. Not shown, but when Δ is 670 MHz, $\delta_m = -12$ MHz. The maximum of the gain curve may not coincide with the FWM resonance because of Raman absorption at the resonance. We experimentally investigate how δ_m varies with certain parameters by keeping Δ fixed. For $\Delta = 1\,\mathrm{GHz}$, $\theta = 3$ mrad, and change of K density from $1.5 \times 10^{12}\,\mathrm{cm}^{-3}$ to $1.7 \times 10^{13}\,\mathrm{cm}^{-3}$, δ_m stayed the same, -3.7 MHz for the probe and -1.7 MHz for the conjugate. On the other hand, changing θ from 5.5 to 2.6 mrad, for the K density of $N = 5.5 \times 10^{12}\,\mathrm{cm}^{-3}$, moves δ_m from -4 MHz to -2.5 MHz. This slight shift to smaller two-photon detuning when the angle is decreasing is the same behavior of δ_m as found for Rb in Ref. [15].

It appears from Fig. 6 that typical curves representing gains versus δ, both calculated and measured, are not symmetric around the maximum. The asymmetric shape of lines might be because of inhomogeneous differential ac Stark shift, since

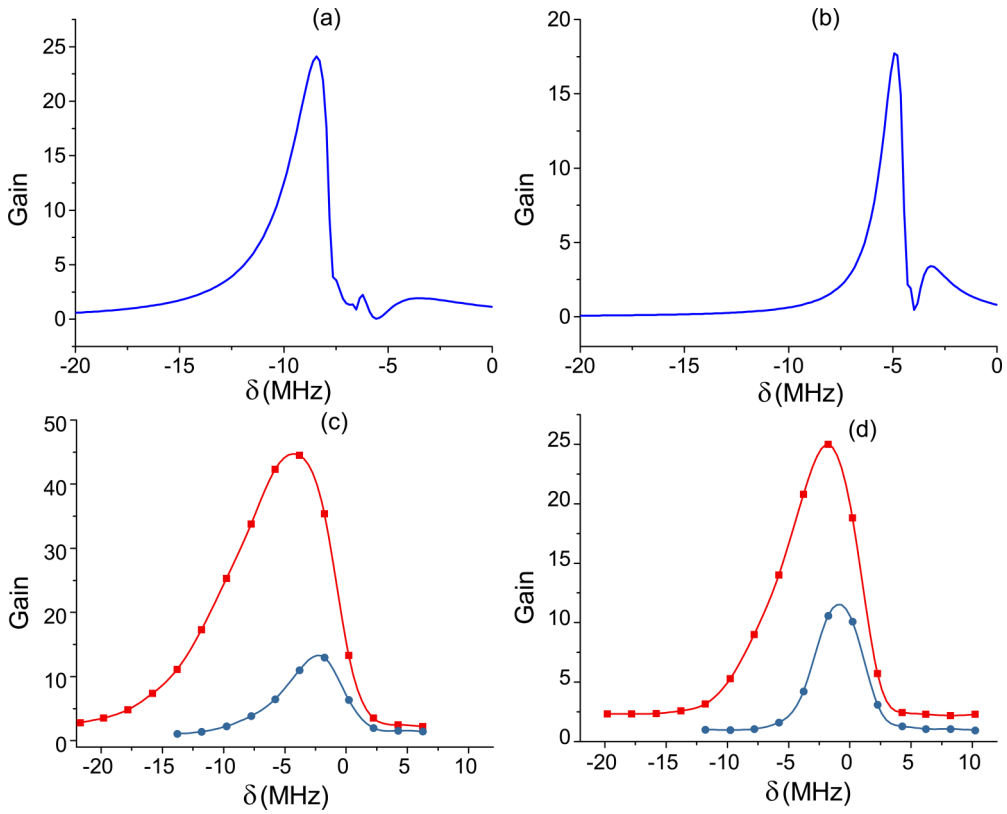

FIG. 6. Gains vs two-photon detuning. (a), (b) Calculations of the conjugate gain. The pump and probe Rabi frequencies are 1.94 GHz and 22.6 MHz, respectively. (c), (d) Experimental results of gains for the probe (solid circles, blue for online version) and the conjugate (solid squares, red for online version). Pump and probe powers are 370 mW and 25˜μW, respectively. (a), (c) $\Delta = 1\,\mathrm{GHz}$, (b), (d) $\Delta = 1.35\,\mathrm{GHz}$. Density $N = 5.5 \times 10^{12}\,\mathrm{cm}^{-3}$, $\theta = 5.5$ mrad.

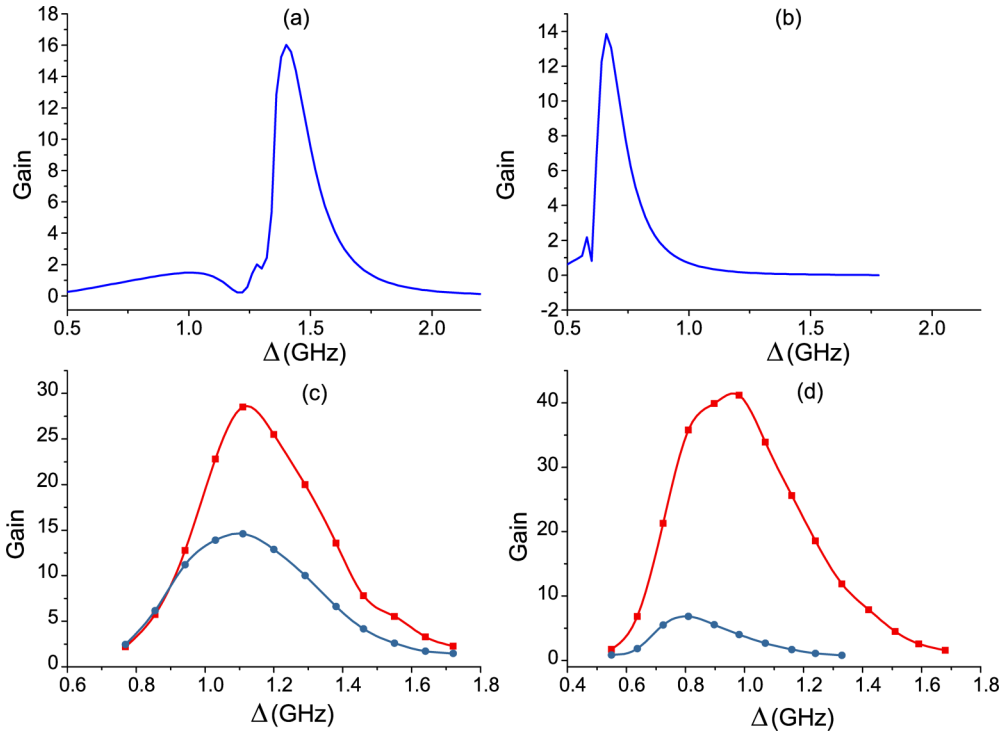

FIG. 7. Gains vs one-photon detuning. (a), (b) calculations of the conjugate gain. (c), (d) experimental results of gains of probe (solid circles, blue for online version) and conjugate (solid squares, red for online version). (a), (c) $\delta = -4$ MHz, (b), (d) $\delta = -8$ MHz. Pump and probe Rabi frequencies, as well as pump and probe powers, K vapor densities, and angle θ are the same as in Fig. 6

atoms in different areas of Gaussian beams experience different laser fields, and thus have different ac shift.

3. Dependence of gains on one-photon detuning

Potassium has larger Doppler broadening than other alkali metals, ∼850 MHz. Width of Doppler line broadening in hot alkali metal vapors determines the range of Δ for large FWM gains. It is between 0.5 and 1 GHz for large gains and best squeezing for Rb and Cs [17,18,30,31].

We have calculated and measured gains versus Δ, with δ and θ as parameters. Presented results are for K vapor density of $N = 5.5 \times 10^{12}$ cm^{-3} (130°C) (see Fig. 7). Parameters in the calculations are the same as for results in Fig. 6. Results in Figs. 7(a) and 7(c) are for $\delta = -4$ MHz, while those in Figs. 7(b) and 7(d) are for $\delta = -8$ MHz. Gains versus Δ are broad, asymmetric curves whose width is 200 MHz for calculated and 400 MHz for measured results.

One-photon detuning for the maximum gain, Δ_m, is close to 1 GHz. We found that Δ_m doesn't change when θ changes if we keep δ the same. On the other hand, for the same angle θ (Fig. 7), Δ_m will have a different value when δ is changed: it is at 0.9 GHz for δ at -8 MHz and can go as far as 1.2 GHz for $\delta \sim 0$ MHz. Because of different detuning, gain of the conjugate is larger then the gain of probe. Large detuning of the probe, beyond the Doppler broadening, minimizes the effect of EIT on the probe absorption.

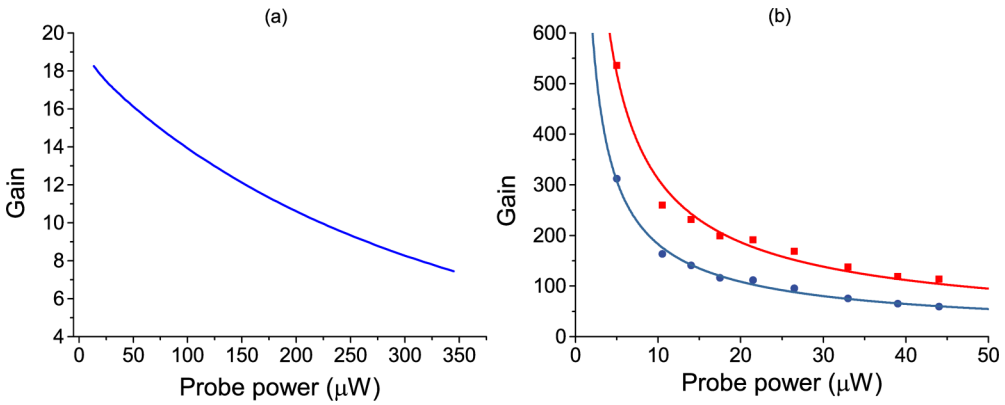

FIG. 8. (a) Calculation of conjugate gain vs probe power. (b) Measurements of probe (solid circles, blue for online version) and conjugate (solid squares, red for online version) gain vs probe power, for $\Delta = 960$ MHz, $\delta = -3.7$ MHz, and cell temperature 130 °C.

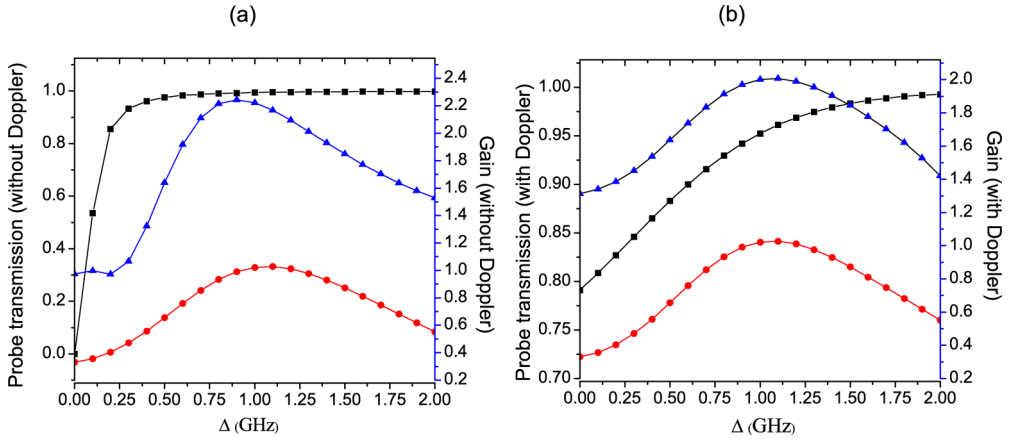

FIG. 9. Calculations of probe transmission (solid squares, black for online version) and gains for probe (solid triangles, blue for online version) and conjugate (solid circles, red for online version): (a) without Doppler averaging; (b) with Doppler averaging.

4. Gain dependence on probe power

Efficiency of FWM in alkali metals depends on the probe power, as presented in Fig. 8, for both calculated and measured values of gains. Evidently the lower the probe power, the higher the gain of both beams. The FWM gain in K vapor can thus be very large. In the experiment, we could not decrease probe below 5 μW because of limited sensitivity of photo diodes. Even without the probe beam at the entrance, with the probe initially in the vacuum state, a strong pump can generate side modes or twin photons [26].

B. Parameters of K vapor for optimum squeezing: Theoretical diagnostics

The numerical model explained above and derived in the Appendix allows us to search for the set of FWM parameters which should provide strong degrees of squeezing in K vapor. It was found, both experimentally and theoretically, in Rb and Cs [16,18,19] that in order to increase the squeezing and noise figure, it is necessary to reduce probe absorption and have modest and similar gains of both probe and conjugate. When plotted as a function of detuning, squeezing is at a maximum when gain is at a maximum. But too large gain results in probe noise that is large due to absorption and losses (fluorescence and nonlinear processes), and depending on gains, one needs FWM parameters that provide optimum probe transmission. Typically, the strongest squeezing is for Δ near the edge of Doppler broadening, when gains are at a maximum and probe transmission at about 90% [16].

We performed thorough analyses of effects of FWM parameters on gains and probe transmission in a search for those that produce maximum gains and large probe transmission at the same time. Results in Fig. 9 show dependence of gains and transmissions on Δ, for K density of 1×10^{12} cm^{-3}, δ -0.5 MHz, and θ 2.8 mrad. Clearly there is the range of Δ near 900 MHz when modest gains are at maximum and probe transmission is high. We recommend this set of parameters for the new measurements of squeezing in K. Results of gains and transmissions are presented with [Fig. 9(a)] and without Doppler averaging [Fig. 9(b)]. Apparently, corrections due to Doppler broadening are small for gains, as found to be the case also for Rb [15], but are considerable for the probe transmission. Results obtained for squeezing in potassium [38] for Δ of 500 MHz and probe transmission below 50% are below values for Rb [16,29] and Cs [19]. Parameters of FMW in Ref. [38] are outside ranges we believe, based on present results, are optimal for squeezing.

V. CONCLUSION

A nonperturbative numerical model was applied to the double-Λ atomic system in potassium vapor, and gains of probe and conjugate were calculated under the conditions of FWM. Results are in agreement with experimental results and show high gains when Δ is slightly larger than the Doppler width and δ is in the range -10–0 MHz. This system is a strong parametric amplifier with gains of several hundred, larger than observed with other alkali-metal atoms for similar pump laser power. On the other hand, potassium is the only alkali metal whose hfs of the ground state is smaller than the Doppler width, i.e., both pump and probe couple simultaneously both ground hfs levels to the excited level.

The model was also used to find parameters of FWM in K vapor that would be optimal for relative amplitude squeezing. In search for these parameters we included results that take into account Doppler averaging of density matrix elements. We have found that the density of 1×10^{12} cm^{-3}, the angle between the pump and the probe $\theta = 2.8$ mrad, while δ and Δ are -0.5 MHz, and ~900 MHz, respectively, and for the pump and the probe Rabi frequencies 1.938 GHz and 23.72 MHz, respectively, are the set of parameters required for strong squeezing in hot potassium vapor.

ACKNOWLEDGMENTS

The authors acknowledge financial help from grants III45016 and OI131038 of the Ministry of Education, Science and Technological Development of Serbia. M.Ć. and I.R. acknowledge support from MP COST (BE) 4103 NQO and IZ73Z0_152511, Joint research projects (SCOPES).

APPENDIX

Far-detuned FWM is treated here as an atomic system with two ground and two excited levels. The pump couples two transitions, $|1>\rightarrow|3>$ and $|2>\rightarrow|4>$, while the probe and conjugate couple $|2>\rightarrow|4>$ and $|4>\rightarrow|1>$, respectively. Transitions to $|3>$ are highly detuned, which justifies introducing another far detuned level $|4>$, with a similarly weak coupling strength from the levels $|1>$ and $|2>$.

The explicit form for the spontaneous emission in Eq. (3) is given by

$$\widehat{SE}=\begin{pmatrix}\Gamma_{1,3}\rho_{33}+\Gamma_{1,4}\rho_{44} & 0 & -\frac{\Gamma_{1,3}+\Gamma_{2,3}}{2}\rho_{13} & -\frac{\Gamma_{1,4}+\Gamma_{2,4}}{2}\rho_{14}\\ 0 & \Gamma_{2,3}\rho_{33}+\Gamma_{2,4}\rho_{44} & -\frac{\Gamma_{1,3}+\Gamma_{2,3}}{2}\rho_{23} & -\frac{\Gamma_{1,4}+\Gamma_{2,4}}{2}\rho_{24}\\ -\frac{\Gamma_{1,3}+\Gamma_{2,3}}{2}\rho_{31} & -\frac{\Gamma_{1,3}+\Gamma_{2,3}}{2}\rho_{32} & -\Gamma_{1,3}\rho_{33}+\Gamma_{2,3}\rho_{33} & -\frac{\Gamma_{1,3}+\Gamma_{2,3}+\Gamma_{1,4}+\Gamma_{2,4}}{2}\rho_{34}\\ -\frac{\Gamma_{1,4}+\Gamma_{2,4}}{2}\rho_{41} & -\frac{\Gamma_{1,4}+\Gamma_{2,4}}{2}\rho_{42} & -\frac{\Gamma_{1,3}+\Gamma_{2,3}+\Gamma_{1,4}+\Gamma_{2,4}}{2}\rho_{43} & -\Gamma_{1,4}\rho_{44}-\Gamma_{2,4}\rho_{44}\end{pmatrix}, \tag{A1}$$

and the relaxation term is

$$\hat{R}=-\gamma\left[\hat{\rho}-\mathrm{diag}\left(\frac{1}{2},\frac{1}{2},0,0\right)\right]-\gamma_{\mathrm{deph}}[\hat{\rho}-\mathrm{diag}(\rho_{11},\rho_{22},\rho_{33},\rho_{44})]. \tag{A2}$$

Optical Bloch equations are

$$\dot{\hat{\rho}}_{11}=\gamma\left(\frac{1}{2}-\rho_{11}\right)+\Gamma_{1,3}\rho_{33}+\Gamma_{1,4}\rho_{44}+\frac{i}{\hbar}\left(E_d^{(+)*}d\rho_{31}-E_d^{(+)}d\rho_{13}+E_c^{(+)*}d\rho_{41}-E_c^{(+)}d\rho_{14}\right), \tag{A3a}$$

$$\dot{\hat{\rho}}_{22}=\gamma\left(\frac{1}{2}-\rho_{22}\right)+\Gamma_{2,3}\rho_{33}+\Gamma_{2,4}\rho_{44}+\frac{i}{\hbar}\left(E_p^{(+)*}d\rho_{32}-E_p^{(+)}d\rho_{23}+E_d^{(+)*}d\rho_{42}-E_d^{(+)}d\rho_{24}\right), \tag{A3b}$$

$$\dot{\hat{\rho}}_{33}=-\rho_{33}\gamma-\Gamma_3\rho_{33}+\frac{i}{\hbar}\left(E_d^{(+)}d\rho_{13}-E_d^{(+)*}d\rho_{31}+E_p^{(+)}d\rho_{23}-E_p^{(+)*}d\rho_{32}\right), \tag{A3c}$$

$$\dot{\hat{\rho}}_{44}=-\rho_{44}\gamma-\Gamma_4\rho_{44}+\frac{i}{\hbar}\left(E_c^{(+)}d\rho_{14}-E_c^{(+)*}d\rho_{41}+E_d^{(+)}d\rho_{24}-E_d^{(+)*}d\rho_{42}\right), \tag{A3d}$$

$$\dot{\hat{\rho}}_{12}=-(\gamma+\gamma_{\mathrm{deph}}+i\Delta_{132})\rho_{12}+\frac{i}{\hbar}\left(E_d^{(+)*}d\rho_{32}-e^{iz\Delta k}E_d^{(+)}d\rho_{14}+e^{iz\Delta k}E_c^{(+)*}d\rho_{42}-E_p^{(+)}d\rho_{13}\right), \tag{A3e}$$

$$\dot{\hat{\rho}}_{13}=-\left(\gamma+\gamma_{\mathrm{deph}}+\frac{\Gamma_3}{2}+i\Delta_{13}\right)\rho_{13}+\frac{i}{\hbar}\left(E_d^{(+)*}d\rho_{33}-E_d^{(+)*}d\rho_{11}+E_c^{(+)*}d\rho_{43}-E_p^{(+)*}d\rho_{12}\right), \tag{A3f}$$

$$\dot{\hat{\rho}}_{14}=-\left(\gamma+\gamma_{\mathrm{deph}}+\frac{\Gamma_4}{2}+i\Delta_{1324}\right)\rho_{14}+\frac{i}{\hbar}\left(E_d^{(+)*}d\rho_{34}-e^{-iz\Delta k}E_d^{(+)*}d\rho_{12}+E_c^{(+)*}d\rho_{44}-E_c^{(+)*}d\rho_{11}\right), \tag{A3g}$$

$$\dot{\hat{\rho}}_{23}=-\left(\gamma+\gamma_{\mathrm{deph}}+\frac{\Gamma_3}{2}+i\Delta_{13}\right)\rho_{23}+\frac{i}{\hbar}\left(E_p^{(+)*}d\rho_{33}-E_d^{(+)*}d\rho_{21}+e^{-iz\Delta k}E_d^{(+)*}d\rho_{43}-E_c^{(+)*}d\rho_{22}\right), \tag{A3h}$$

$$\dot{\hat{\rho}}_{24}=-\left(\gamma+\gamma_{\mathrm{deph}}+\frac{\Gamma_4}{2}+i\Delta_{1324}\right)\rho_{24}+\frac{i}{\hbar}\left(E_d^{(+)*}d\rho_{44}-E_d^{(+)*}d\rho_{22}+e^{iz\Delta k}E_p^{(+)*}d\rho_{34}-e^{iz\Delta k}E_c^{(+)*}d\rho_{21}\right), \tag{A3i}$$

$$\dot{\hat{\rho}}_{34}=-\left(\gamma+\gamma_{\mathrm{deph}}+\frac{\Gamma_3}{2}+\frac{\Gamma_4}{2}+i\Delta_{1324}-i\Delta_{13}\right)\rho_{34}+\frac{i}{\hbar}\left(E_d^{(+)}d\rho_{14}-e^{-iz\Delta k}E_d^{(+)*}d\rho_{32}+e^{iz\Delta k}E_p^{(+)}d\rho_{24}-E_c^{(+)*}d\rho_{31}\right). \tag{A3j}$$

Here Δk is the phase mismatch defined as $\Delta k=2k_d-k_p-k_c$, where k_d is the pump wave vector. $\Gamma_{i,j}$ is the decay rate from level j to level i, while $\Gamma_i=\Gamma_{i,1}+\Gamma_{i,2}$. $\gamma=10^5$ Hz is spontaneous decay from the excited state, and $\gamma_{\mathrm{deph}}=0$ is the dephasing decay rate.

[1] L. M. Duan, M. D. Lukin, J. I. Cirac, and P. Zoller, Nature (London) **414**, 413 (2001).

[2] C. Shu, P. Chen, T. K. A. Chow, L. Zhu, Y. Xiao, M. Loy, and S. Du, Nat. Commun. **7**, 12783 (2016).

[3] R. C. Pooser, A. M. Marino, V. Boyer, K. M. Jones, and P. D. Lett, Phys. Rev. Lett. **103**, 010501 (2009).

[4] V. Boyer, C. F. McCormick, E. Arimondo, and P. D. Lett, Phys. Rev. Lett. **99**, 143601 (2007).

[5] J. Okuma, N. Hayashi, A. Fujisawa, and M. Mitsunaga, Opt. Lett. **34**, 1654 (2009).

[6] Y. Wu and X. Yang, Phys. Rev. A **70**, 053818 (2004).

[7] J. Wu, Y. Liu, D. S. Ding, Z. Y. Zhou, B.-S. Shi, and G.-C. Guo, Phys. Rev. A **87**, 013845 (2013).

[8] R. M. Camacho, P. K. Vudyasetu, and J. C. Howell, Nat. Photon. **3**, 103 (2009).

[9] A. Eilam, A. D. Wilson-Gordon, and H. Friedmann, Opt. Lett. **33**, 1605 (2008).

[10] D. S. Ding, Z. Y. Zhou, B. S. Shi, X. B. Zou, and G. C. Guo, Opt. Express **20**, 11433 (2012).
[11] A. Leszczyński, M. Parniak, and W. Wasilewski, Opt. Express **25**, 284 (2017).
[12] K. I. Harada, K. Mori, J. Okuma, N. Hayashi, and M. Mitsunaga, Phys. Rev. A **78**, 013809 (2008).
[13] K. I. Harada, T. Kanbashi, M. Mitsunaga, and K. Motomura, Phys. Rev. A **73**, 013807 (2006).
[14] C. F. McCormick, V. Boyer, E. Arimondo, and P. D. Lett, Opt. Lett. **32**, 178 (2007).
[15] M. T. Turnbull, P. G. Petrov, C. S. Embrey, A. M. Marino, and V. Boyer, Phys. Rev. A **88**, 033845 (2013).
[16] C. F. McCormick, A. M. Marino, V. Boyer, and P. D. Lett, Phys. Rev. A **78**, 043816 (2008).
[17] Q. Glorieux, L. Guidoni, S. Guibal, J. P. Likforman, and T. Coudreau, Phys. Rev. A **84**, 053826 (2011).
[18] M. Jasperse, L. D. Turner, and R. E. Scholten, Opt. Express **19**, 3765 (2011).
[19] M. Guo, H. Zhou, D. Wang, J. Gao, J. Zhang, and S. Zhu, Phys. Rev. A **89**, 033813 (2014).
[20] V. Boyer, A. M. Marino, R. C. Pooser, and P. D. Lett, Science **321**, 544 (2008).
[21] A. M. Marino, R. C. Pooser, V. Boyer, and P. D. Lett, Nature (London) **457**, 859 (2009).
[22] S. L. Braunstein and P. van Loock, Rev. Mod. Phys. **77**, 513 (2005).
[23] A. Gaeta, M. Gruneisen, and R. Boyd, IEEE J. Quantum Electron. **22**, 1095 (1986).
[24] M. D. Lukin, P. R. Hemmer, M. Loffler, and M. O. Scully, Phys. Rev. Lett. **81**, 2675 (1998).
[25] Q. Glorieux, R. Dubessy, S. Guibal, L. Guidoni, J. P. Likforman, T. Coudreau, and E. Arimondo, Phys. Rev. A **82**, 033819 (2010).
[26] G. S. Agarwal, Phys. Rev. A **34**, 4055 (1986).
[27] P. Kolchin, Phys. Rev. A **75**, 033814 (2007).
[28] B. Ai, D. S. Glassner, R. J. Knize, and J. P. Partanen, Appl. Phys. Lett. **64**, 951 (1994).
[29] R. C. Pooser, A. M. Marino, V. Boyer, K. M. Jones, and P. D. Lett, Opt. Express **17**, 16722 (2009).
[30] Z. Qin, J. Jing, J. Zhou, C. Liu, R. C. Pooser, Z. Zhou, and W. Zhang, Opt. Lett. **37**, 3141 (2012).
[31] G. Adenier, D. Calonico, S. Micalizio, N. Samantaray, I. Degiovanni, and I. R. Berchera, Int. J. Quantum Inform. **14**, 1640014 (2016).
[32] W. V. Davis, M. Kauranen, E. M. Nagasako, R. J. Gehr, A. L. Gaeta, R. W. Boyd, and G. S. Agarwal, Phys. Rev. A **51**, 4152 (1995).
[33] B. Zlatković, A. J. Krmpot, N. Šibalić, M. Radonjić, and B. M. Jelenković, Laser Phys. Lett. **13**, 015205 (2016).
[34] J. A. Kleinfeld and A. D. Streater, Phys. Rev. A **53**, 1839 (1996).
[35] D. S. Glassner and R. J. Knize, Appl. Phys. Lett. **66**, 1593 (1995).
[36] M. Katharakis, N. Merlemis, A. Serafetinides, and T. Efthimiopoulos, J. Phys. B **35**, 4969 (2002).
[37] M. Y. Lanzerotti, R. W. Schirmer, and A. L. Gaeta, Appl. Phys. Lett. **69**, 1199 (1996).
[38] J. D. Swaim and R. T. Glasser, Phys. Rev. A **96**, 033818 (2017).
[39] D. A. Steck, Quantum and Atom Optics, http://steck.us/teaching (revision 0.12.0, 16 May 2017).
[40] D. McKay, Potassium 5p line data, http://fermionlattice.wdfiles.com/local–files/papers/5P_structure, 2009.